Supplementary Information (SI) for CrystEngComm.

Chemical Vapor Transport Synthesis of One-Dimensional V_2PS_{10} and Its Application in Miniaturized UV Sensors

Jinsu Kang[a,†], Sooheon Cho[a,†], Xiaojie Zhang[a], Bom Lee[a], Byung Joo Jeong[a], Kyung Hwan Choi[b], Jiho Jeon[b], Sang Hoon Lee[a], Jae-Hyuk Park[a], Sang Hyuk Kim[,a], Hak Ki Yu[*,c], and Jae-Young Choi[*,a,d]*

[a]School of Advanced Science Materials and Engineering, Sungkyunkwan University, Suwon 16419, Republic of Korea

[b]SKKU Advanced Institute of Nanotechnology (SAINT), Sungkyunkwan University, Suwon 16419, Republic of Korea

[c]Department of Materials Science and Engineering & Department of Energy Systems Research, Ajou University, Suwon 16499, Republic of Korea

[d]KIST-SKKU Carbon-Neutral Research Center, Sungkyunkwan University, Suwon 16419, Republic of Korea

#: authors equally contributed

Corresponding authors e-mail:
sh47kim@skku.edu & hakkiyu@ajou.ac.kr & jy.choi@skku.edu

TABLE OF CONTENTS

SUPPORTING FIGURES

Morphology of V_2PS_{10} nanowire synthesized by various reaction condition

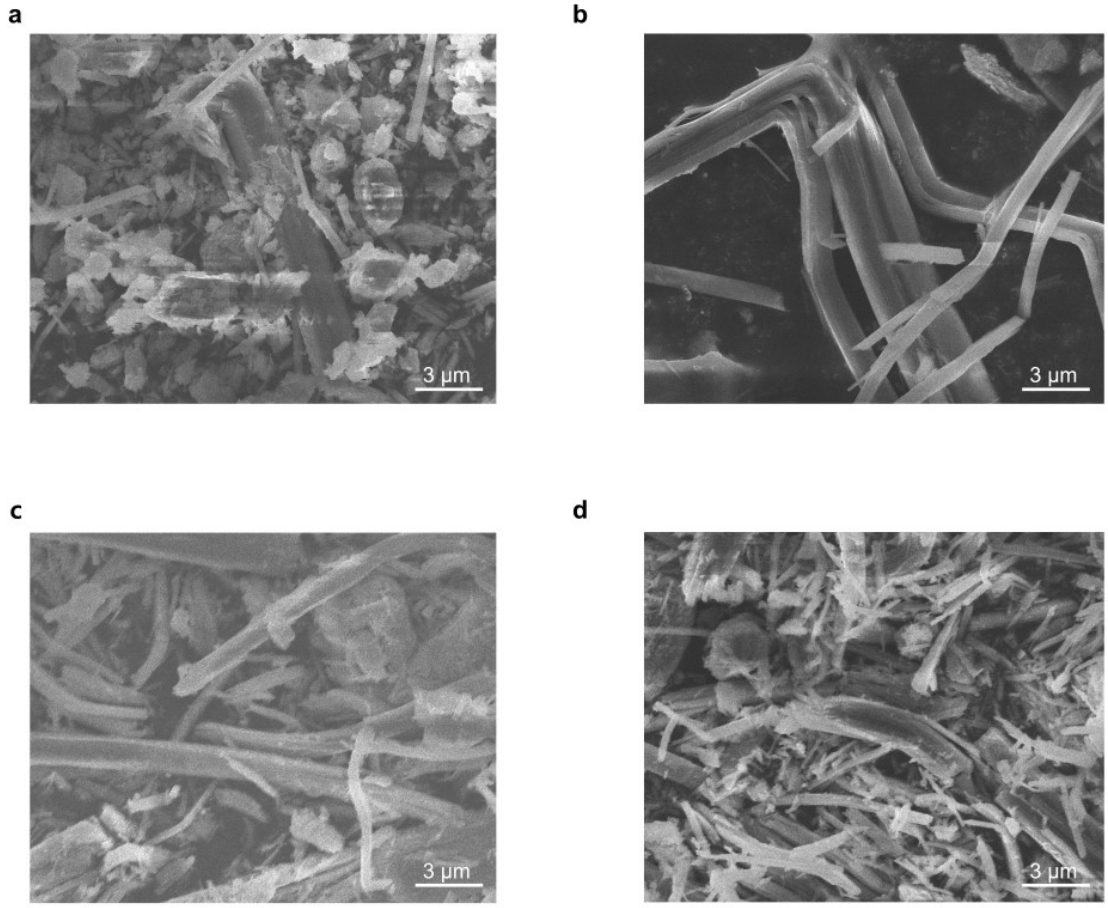

Fig. S1 SEM image of V_2PS_{10} nanowire synthesized by various reaction condition. (a) Using VS_4 as intermediate phase precursor instead of Vanadium precursor and heated to 450°C for 3 days. (b), (c), and (d) Using V, P and S as precursor. (b) 500°C for 3 days. (c) 480°C for 7 days. (d) 500°C for 7 days.

The expanded XRD peaks of V_2PS_{10} powder under various synthesis conditions

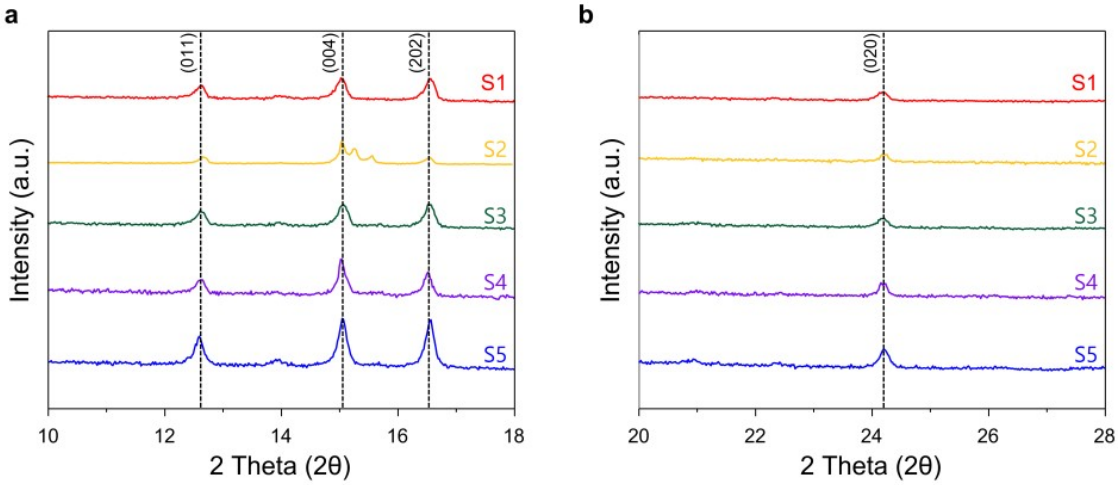

Fig. S2 The expanded XRD peaks in Figure 2b. (a) $10^{\circ} < 2\theta < 18^{\circ}$. (b) $20^{\circ} < 2\theta < 28^{\circ}$.

The result of Rietveld refinement of the XRD graph of the V_2PS_{10} powder by CVT method

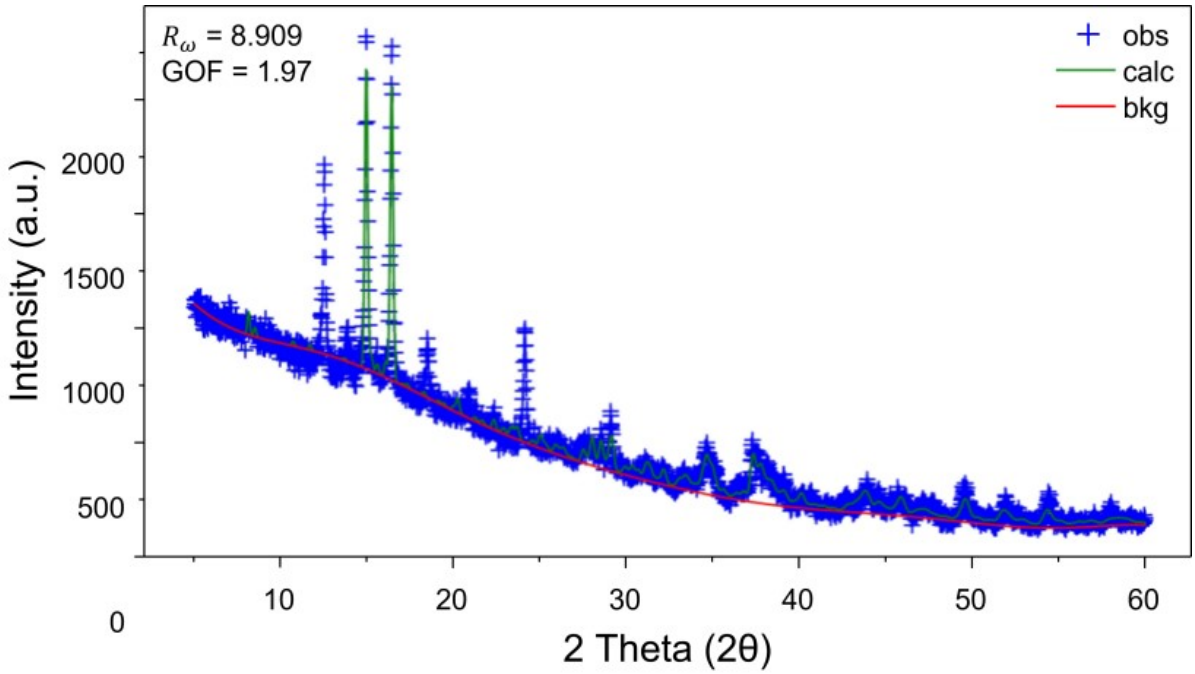

※ $R_\omega = \sqrt{\frac{\sum_i \omega_i (y_{obs,\,i} - y_{calc,i})^2}{\sum_i \omega_i y_{obs,\,i}^2}}$,

R_ω = *weighted residual factor*

※ $GOF = \frac{R_\omega}{R_{expected}} = \sqrt{\frac{\sum_i \omega_i (y_{obs,\,i} - y_{calc,i})^2}{N - P}}$,

$R_{expected}$ = *The expected R value, which represents the ideal level of data fit.*

N = *The total number of data points.*

P = *The number of refined parameters.*

Fig. S3 The results of Rietveld refinement of the XRD graph under S5 condition.

Morphology and atomic ratio of the V_2PS_{10} nanowires synthesized by CVT method

a

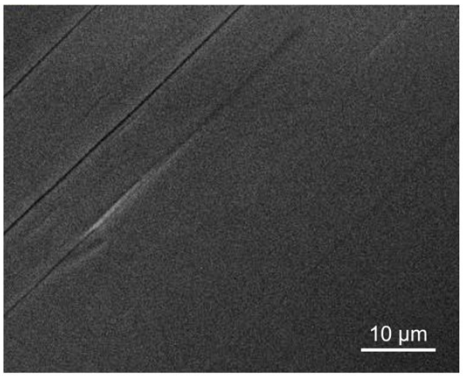

b

Element	At%	Ratio
V K	7.85	2
P K	4.72	1.20
S K	43.49	11.08

Fig. S4 (a) SEM image of the V_2PS_{10} single crystal nanowire synthesized by CVT method. (b) The ratio of the elements obtained by EDS.

Dispersion of the V_2PS_{10} nanowires with various solvent

Material	V_2PS_{10}							
Sonication	3hr							
RPM	6000							
Solvent	Toluene	Chloroform	Acetone	IPA	Ethanol	DMF	NMP	DI
After Sonication	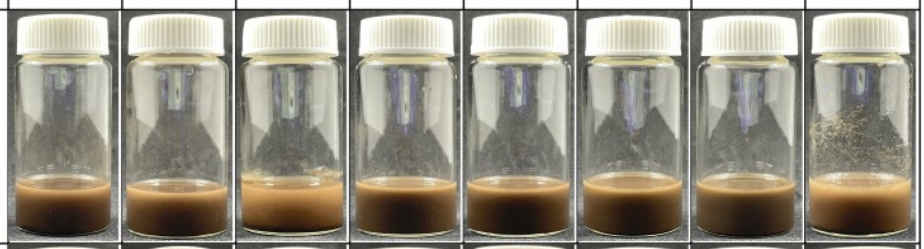							
After Centrifugation	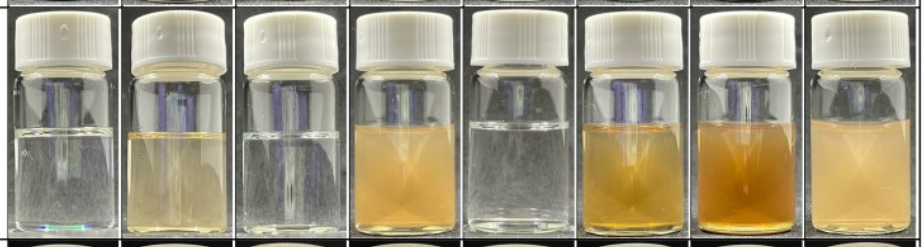							
Tyndall Effect	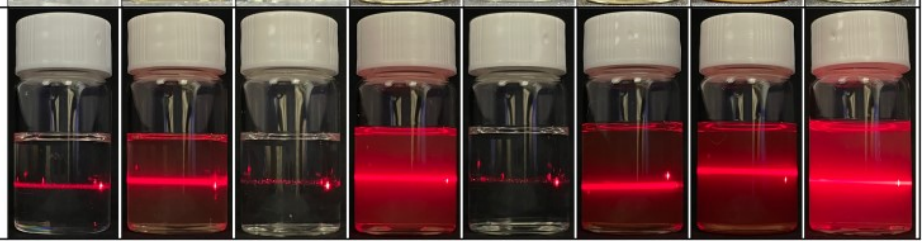							

Fig. S5 Tyndall effect of V_2PS_{10} solutions dispersed in various solvents.

Absorbance graph according to dielectric constant and surface tension of various solvents

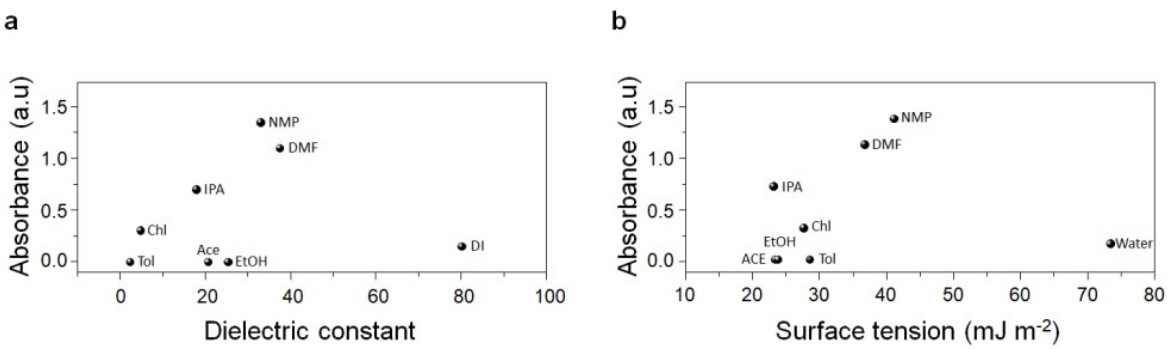

Fig. S6 (a) Dielectric constant vs Absorbance graph of dispersed solvent. (b) Surface tension vs Absorbance graph of dispersed solvent.

Comparison of rise/decay time and on/off ratio of various 1D material-based UV sensors

material	year	rise time (ms)	decay time (ms)	on/off ratio	Ref.
ZnS nanowire	2017	90	70	19173	1
WO_3	2023	75	69	-	2
$CsCu_2I_3$	2021	160	320	3150	3
ZnO nanowire	2017	450	60	100	4
TiO_2 nanowire	2018	400	100	2000	5
V_2PS_{10}	2024	60.1	214.4	16395	This work

Table. S1 Comparison of rise/decay time and on/off ratio of various 1D material-based UV sensors

Reference

[1] Q. An, X. Meng, K. Xiong, Y. Qiu, Self-powered ZnS Nanotubes/Ag Nanowires MSM UV Photodetector with High On/Off Ratio and Fast Response Speed, Sci. Rep. 7 (2017) 4885.

[2] A. Yadav, L. Goswami, P. Vashishtha, A. Sharma, P. Goswami, G. Gupta, Highly responsive WO3 based UV-Vis photodetector, Sensors Actuators A Phys. 362 (2023) 114641.

[3] X. Zhou, L. Zhang, Y. Huang, Z. Zhou, W. Xing, J. Zhang, F. Zhou, D. Zhang, F. Zhao, Enhanced Responsivity of CsCu2I3 Based UV Detector with CuI Buffer-Layer Grown by Vacuum Thermal Evaporation, Adv. Optical Mater. 9 (2021) 2100889.

[4] L. Li, H. Jiang, X. Han, Z. Zhan, H. Du, W. Lu, Z. Li, Z. Tao, Y. Fan, Optimizing growth of ZnO nanowire networks for high-performance UV detection, Ceramics International 43 (2017) 15978–15985.

[5] Y. Zou, Y. Zhang, Y. Hu, H. Gu, Ultraviolet Detectors Based on Wide Bandgap Semiconductor Nanowire: A Review, Sensors 18 (2018) 2072.